Macromolecules

ARTICLE

pubs.acs.org/Macromolecules

New Donor−Acceptor Random Copolymers with Pendent Triphenylamine and 1,3,4-Oxadiazole for High-Performance Memory Device Applications

Yi-Kai Fang,[†,⊥] Cheng-Liang Liu,[‡,⊥] Guei-Yu Yang,[§] Po-Cheng Chen,[§] and Wen-Chang Chen*[,†,§]

[†]Institute of Polymer Science and Engineering, National Taiwan University, Taipei, Taiwan 106

[‡]Department of Organic Device Engineering, Yamagata University, Yonezawa, Yamagata 992-8510, Japan

[§]Department of Chemical Engineering, National Taiwan University, Taipei, Taiwan 106

Supporting Information

ABSTRACT: We report the synthesis and resistive-type switching memory characteristics based on new P(VTPA$_x$BOXD$_y$) and P(CNVTPA$_x$BOXD$_y$) random copolymers containing different donor/acceptor ratios (8/2, 5/5, and 2/8) of pendent electron-donating 4-vinyltriphenylamine (VTPA) or 4,4′-dicyano-4″-vinyltriphenylamine (CNVTPA) and electron-withdrawing 2-(4-vinylbiphenyl)-5-(4-phenyl)-1,3,4-oxadiazole (BOXD). The effects of donor/acceptor ratios and cyano side group on the memory characteristics were explored and compared with properties of homopolymers, PVTPA, PCNVTPA, and POXD. The distinct electrical current−voltage (I−V) characteristics of the ITO/P(VTPA$_x$BOXD$_y$)/Al device changed from volatile memory to insulator depending on the relative donor/acceptor ratios. The ITO/P(VTPA$_8$BOXD$_2$) or PVTPA/Al device exhibited SRAM or DRAM behavior with an ON/OFF current ratio of 10^7−10^8. However, no switching phenomena were observed for a higher BOXD ratio. Moreover, the devices could endure 10^8 cycles under a voltage pulse and show a long retention time for at least 10^4 s under constant voltage stress. The low-lying HOMO energy level of BOXD was employed as the hole-blocking moiety as the charge transport occurred between the neighboring triphenylamine units. The charge trapping/spontaneously back-transferring of trapped carriers controlled the switching behavior. On the other hand, all the P(CNVTPA$_x$BOXD$_y$) memory devices exhibited nonvolatile nature with NDR behavior due to the preferred interaction of Al atoms with the cyano group. Here, the results demonstrated that the pendent polymers with specific donor−acceptor chromophores could tune the memory switching characteristics for advanced electronic device applications.

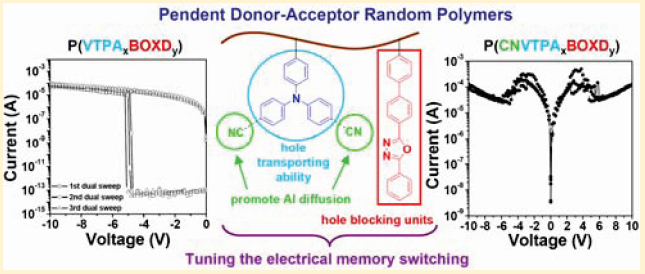

INTRODUCTION

Donor−acceptor (D−A) polymer systems have widely investigated for organic electronics, such as light-emitting diodes,[1,2] photovoltaic cells,[3−16] field-effect transistors,[11−18] and memory devices.[19−21] They provide the advantages of flexibility, low cost, solution processability, and three-dimensional stacking capability as compared with inorganic counterparts.[1−21]

Because of the stable electron-donating nitrogen atom in the triphenylamine (TPA),[22,23] the TPA-based D−A polymers were developed for various electronic applications.[24−33] In addition, the energy level of TPA-based polymers can be chemically tuned through the different strength of electron acceptors to meet the requirement of original molecular design for specific organic electronics. For example, functional polyimides (PIs) containing electron-donating TPA moieties and electron-withdrawing phthalimide moieties were demonstrated for the device application of dynamic random access memory (DRAM), static random access memory (SRAM), write-once-read-many times (WORM), and flash memory via an external voltage bias or pulse.[24−28] Soluble TPA-based polyazomethine grafted with graphene oxide acceptors was prepared for bistable flash memory device.[29] Besides, side-chain TPA−perylene block copolymers influenced the HOMO energy level and microphase-separated morphologies, which affected the solar cell performance significantly.[30,31]

We are particularly interested in the design and synthesis of D−A polymer systems for resistive-type memory device applications.[27,34−37] The reported D−A materials system for the volatile and nonvolatile memory devices included small molecules,[38,39] conjugated polymers,[40−42] nonconjugated polymers with D/A chromophores (functional polyimide[24−29,34] or pendent polymers[36,43,44]), and polymer nanocomposites (metal nanoparticle,[45,46] fullerene,[37,47] carbon nanotube,[48] or graphene oxide[29] embedded). The original switching mode of memory devices were operated through several proposed mechanisms such as the trapping/detrapping of charges, charge transfer effect, and filamentary conduction, as summarized by Kang and co-workers.[19]

Received: January 27, 2011
Revised: March 4, 2011
Published: March 25, 2011

Scheme 1. Synthesis of Random Copolymers P(VTPA$_x$BOXD$_y$) and P(CNVTPA$_x$BOXD$_y$)

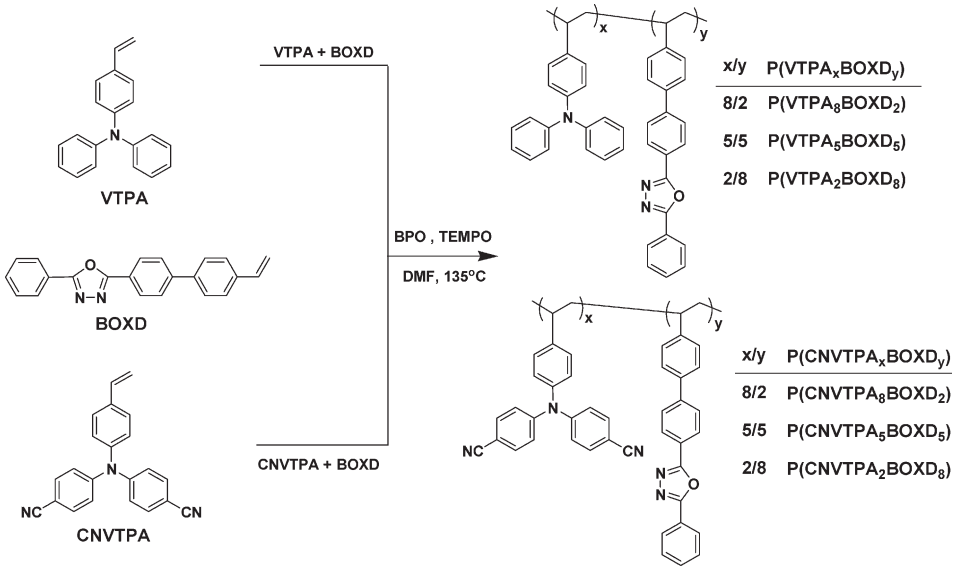

The D−A copolymers comprising TPA and triazine or oxadiazole were only applied for light-emitting diode applications.[22,23] However, the memory characteristics of such copolymers have not been fully explored yet.

In this study, we report the synthesis of nonconjugated random copolymers with pendant donor and acceptor groups for memory device applications. The used electron-donating moiety was 4-vinyltriphenylamine (VTPA) or 4,4′-dicyano-4″-vinyltriphenylamine (CNVTPA) while the electron-withdrawing moiety was the 2-(4-vinylbiphenyl)-5-(4-phenyl)-1,3,4-oxadiazole (BOXD) group. Here, various pendent random copolymers P(VTPA$_x$BOXD$_y$) or P(CNVTPA$_x$BOXD$_y$) with different D/A ratios were synthesized by the nitroxide-mediated free radical polymerization (NMRP). The thermal, optical, and electrochemical properties of the new synthesized copolymers were characterized and compared with those of the corresponding homopolymers, PVTPA, PCNTPA, and PBOXD. The memory behavior was measured by a simple sandwich device configuration consisted of spin-coated polymer films between ITO and Al electrodes. From the related energy levels of interface, the HOMO values and hole-injection ability were varied through the pendent TPA derivatives while the low-lying HOMO energy level of BOXD electron acceptor can block the transport of charge carriers. The experimental results suggested that the observed switching behavior was determined by D/A ratio through the ability of charge trapping/back-transferring of trapped charges and metal diffusion effect.

EXPERIMENTAL SECTION

Materials. Benzoyl peroxide (BPO) and 2,2,6,6-tetramethylpiperidine 1-oxyl (TEMPO) were obtained from Acros (Geel, Begium). Anhydrous toluene and dimethylformamide (DMF) were obtained from TEDIA (Fairfield, CT). All the chemicals were used as received and without further purification. Tetrabutylammonium perchlorate (TBAP, TCI) was recrystallized twice from ethyl acetate and then dried in vacuum prior to use. The monomers of 4-vinyltriphenylamine (VTPA), 4,4′-dicyano-4″-vinyltriphenylamine (CNVTPA), and 2-(4-vinylbiphenyl)-5-(4-phenyl)-1,3,4-oxadiazole (BOXD) were prepared according to the literature.[49,50] The detailed synthetic procedures of the homopolymers, PVTPA, PCNTPA, and PBOXD, are reported in the Supporting Information.

General Polymerization Procedure of Random Copolymers. The procedure of random copolymers on based nitroxide-mediated free radical polymerization (NMRP) is shown in Scheme 1. The reaction process comprises a mixture of VTPA (or CNVTPA) and BOXD monomers, free radical initiator (BPO), stable free radical (TEMPO), and DMF in glass tube with a magnetic stirring bar. The mixture was degassed and backfilled with N_2 three times, sealed under N_2 flow, and placed in 135 °C oil bath for 4 h. After cooling, DMF was added to dissolve the polymers, and the solution was reprecipitated into methanol. The polymers were used for further purification by Soxhlet extraction in acetone. The copolymers were finally dried under vacuum at 60 °C overnight. The weight-average molecular weights (M_w) of the copolymers, obtained by GPC using THF (for P(VTPA$_x$BOXD$_y$)) or DMF (for P(VTPA$_x$BOXD$_y$)) as the elute and polystyrene as standards, were 12 700−16 500 and 24 000−29 600 g/mol with the polydispersity index (PDI) of 1.24−1.37 and 1.17−1.31, respectively. The relative ratios of D/A segments in the random copolymers were estimated form elemental analysis. The reaction compositions and characterization are described as the following:

P(VTPA$_8$BOXD$_2$): 474 mg of VTPA (1.74 mmol), 141 mg of BOXD (0.47 mmol), 6.6 mg of BPO (0.028 mmol), 5.0 mg of TEMPO (0.034 mmol), and DMF (1 mL) were used to afford 144 mg of gray solid (23.5%). ^{1}H NMR ($CDCl_3$), δ (ppm): 6.21−8.19 (br, 27H, Ar−H), 1.26−2.30 (br, 6H, $-CH_2-CH-$). Anal. Calcd for $[(C_{20}H_{17}N)_{0.8} + (C_{22}H_{16}N_2O)_{0.2}]$: C, 86.76; H, 6.09; N, 5.95. Found: C, 84.18; H, 5.99; N, 5.49. M_w and PDI estimated from GPC are 14 700 and 1.34, respectively.

P(VTPA$_5$BOXD$_5$): 287 mg of VTPA (1.05 mmol), 343 mg of BOXD (1.14 mmol), 6.4 mg of BPO (0.026 mmol), 5.5 mg of TEMPO (0.033 mmol), and DMF (1 mL) were used to afford 165 mg of white solid (26.2%). ^{1}H NMR ($CDCl_3$) δ (ppm): 6.21−8.21 (br, 27H, Ar−H), 1.31−2.43 (6H, $-CH_2-CH-$). Anal. Calcd for $[(C_{20}H_{17}N)_{0.5} + (C_{22}H_{16}N_2O)_{0.5}]$: C, 84.38; H, 5.85; N, 7.03. Found: C, 82.68; H, 5.33; N, 6.75. M_w and PDI estimated from GPC are 15 000 and 1.37, respectively.

P(VTPA$_2$BOXD$_8$): 112 mg of VTPA (0.41 mmol), 540 mg of BOXD (1.80 mmol), 6.30 mg of BPO (0.026 mmol), 5.2 mg of TEMPO (0.034 mmol), and DMF (1 mL) were used to afford 106 mg of white solid

(16.4%). ^{1}H NMR ($CDCl_3$) δ (ppm): 6.32−8.23 (br, 27H, Ar−H), 1.36−2.67 (6H, $-CH_2-CH-$). Anal. Calcd for $[(C_{20}H_{17}N)_{0.2} + (C_{22}H_{16}N_2O)_{0.8}]$: C, 82.24; H, 5.64; N, 7.99. Found: C, 81.29; H, 5.36; N, 7.97. M_w and PDI estimated from GPC are 12 700 and 1.24, respectively.

P(CNVTPA$_8$BOXD$_2$): 503 mg of CNVTPA (1.57 mmol), 97 mg of BOXD (0.39 mmol), 6.67 mg of BPO (0.028 mmol), 5.0 mg of TEMPO (0.036 mmol), and DMF (1 mL) were used to afford 144 mg of gray solid (22.0%). ^{1}H NMR ($CDCl_3$) δ (ppm): 6.62−8.23 (br, 25H, Ar−H), 1.43−2.63 (br, 6H, $-CH_2-CH-$). Anal. Calcd for $[(C_{22}H_{15}N_3)_{0.8} + (C_{22}H_{16}N_2O)_{0.2}]$: C, 81.37; H, 4.69; N, 12.78. Found: C, 80.10; H, 5.05; N, 12.52. M_w and PDI estimated from GPC are 25 000 and 1.17, respectively.

P(CNVTPA$_5$BOXD$_5$): 338 mg of CNVTPA (1.06 mmol), 262 mg of BOXD (1.06 mmol), 7.10 mg of BPO (0.029 mmol), 5.95 mg of TEMPO (0.038 mmol), and DMF (1 mL) were used to afford 143 mg of gray solid (23.8%). ^{1}H NMR ($CDCl_3$) δ (ppm): 1.32−2.16 (br, 6H, $-CH_2-CH-$), 6.41−8.18 (br, 25H, Ar−H). Anal. Calcd for $[(C_{22}H_{15}N_3)_{0.5} + (C_{22}H_{16}N_2O)_{0.5}]$: C, 80.04; H, 4.74; N, 12.29. Found: C, 78.5; H, 5.10; N, 11.93. M_w and PDI estimated from GPC are 25 640 and 1.19, respectively.

P(CNVTPA$_2$BOXD$_8$): 147 mg of CNVTPA (0.457 mmol), 453 mg of BOXD (1.82 mmol), 6.92 mg of BPO (0.028 mmol), 5.80 mg of TEMPO (0.037 mmol), and DMF (1 mL) were used to afford 151 mg of gray solid (25.2%). ^{1}H NMR ($CDCl_3$) δ (ppm): 6.32−8.19 (br, 25H, Ar−H), 1.33−2.15 (br, 6H, $-CH_2-CH-$). Anal. Calcd for $[(C_{22}H_{15}N_3)_{0.2} + (C_{22}H_{16}N_2O)_{0.8}]$: C, 78.51; H, 4.79; N, 12.72. Found: C, 77.38; H, 5.13; N, 11.39. M_w and PDI estimated from GPC are 28 000 and 1.31, respectively.

Characterization. ^{1}H NMR spectra were measured on a Bruker Avance 300 MHz FT-NMR spectrometer. Gel permeation chromatographic (GPC) analysis was performed on a Lab Alliance RI2000 instrument (one column, MIXED-D from Polymer Laboratories) connected with one refractive index detector from Schambeck SFD Gmbh. All GPC analyses were performed on polymer/THF (or DMF) solution at a flow rate of 1 mL/min at 40 °C (70 °C) and calibrated with polystyrene standards. Elemental analyses were performed with a Heraeus VarioEL-III-NCSH instrument.

Thermogravimetric analysis (TGA) was conducted with a PerkinElmer Pyris 1 TGA at a heating rate of 20 °C/min. Differential scanning calorimetry (DSC) measurements were performed under a nitrogen atmosphere at a heating rate of 20 °C/min from −50 to 250 °C using a TA Instruments DSC-Q100. Electrochemistry was performed with a CHI 611B electrochemical analyzer and a three-electrode cell in which ITO (polymer films area about 0.7 × 0.5 cm^2) was used as a working electrode. A platinum wire was used as an auxiliary electrode. All cell potentials were taken with the use of a homemade Ag/AgCl, KCl(sat.) reference electrode. Absorption spectra were measured with a Hitachi U4100 UV−vis−NIR spectrophotometer. The thickness of the polymer film was measured with a Microfigure Measuring Instrument (Surfcorder ET3000, Kosaka Laboratory Ltd.).

Fabrication and Characterization of Polymer Memory Devices. The memory devices were fabricated on the ITO glass with the configuration of ITO/polymer/Al. Before the deposition of the polymer layer, the glass was precleaned by ultrasonication with water, isopropanol, and acetone, each for 15 min. Then, 20 or 35 mg/mL of polymer solution in chlorobenzene or dimethylacetamide (DMAc) solution was spin-coated onto the precleaned ITO glass at speed rates of 1000 and 800 rpm for 60 and 120 s, respectively, and baked at 150 °C for 10 min under vacuum. The polymer film thickness was determined to be around 70 nm. Finally, a 300 nm thick Al top electrode (recorded device units of 0.5 × 0.5 mm^2 in size) was thermally evaporated through the shadow mask at a pressure of 10^{-7} Torr with a uniform depositing rate of 3−5 Å/s. The electrical characterization of the memory device

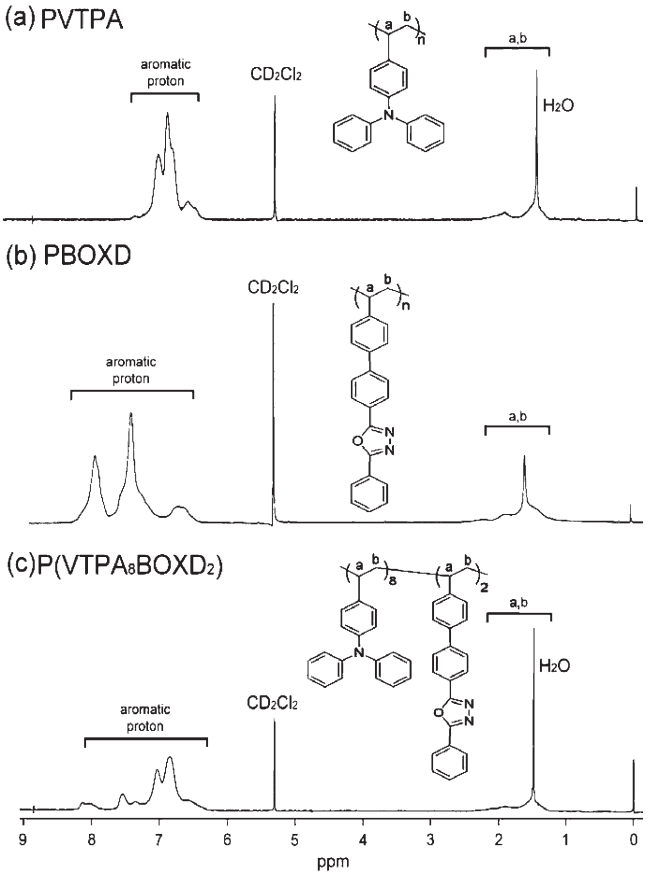

Figure 1. ^{1}H NMR spectra of (a) PVTPA, (b) PBOXD, and (c) P(VTPA$_8$BOXD$_2$) in CD_2Cl_2.

was performed by a Keithley 4200-SCS semiconductor parameter analyzer equipped with a Keithley 4205-PG2 arbitrary waveform pulse generator. Al was used as the anode and ITO was set as the cathode (maintained as common) during the voltage sweep with a step of 0.1 V. The probe tip used 10 μm diameter tungsten wire attached to a tinned copper shaft with a point radius <0.1 μm (GGB Industries, Inc.). All the device fabrication and electronic measurement were performed in a glovebox.

Computational Methodology. Molecular calculations studied in this work have been performed with Gaussian 03 program package.[51] Equilibrium ground state geometry and electronic properties were optimized by means of the density functional theory (DFT) method at the B3LYP level of theory (Beckes-style three-parameter density functional theory using the Lee−Yang−Parr correlation functional) with the 6-31G(d) basic set.

RESULTS AND DISCUSSION

Polymer Characterization. Random copolymers of P(VTPA$_x$BOXD$_y$) and P(CNVTPA$_x$BOXD$_y$) with varying donor (VTPA or CNVTPA)/acceptor (BOXD) ratios were synthesized employing the NMRP method. The subscripts (x or y) indicate the molar ratio of donor or acceptor moiety. Here, the structures of synthetic random copolymers and homopolymers were confirmed by ^{1}H NMR spectra and elemental analysis. As shown Figure 1, the spectrum of P(VTPA$_8$BOXD$_2$) random copolymer indicates that the signals in 1.26−2.30 and 6.21−8.19 ppm are attributed to the vinyl protons and aromatic protons,

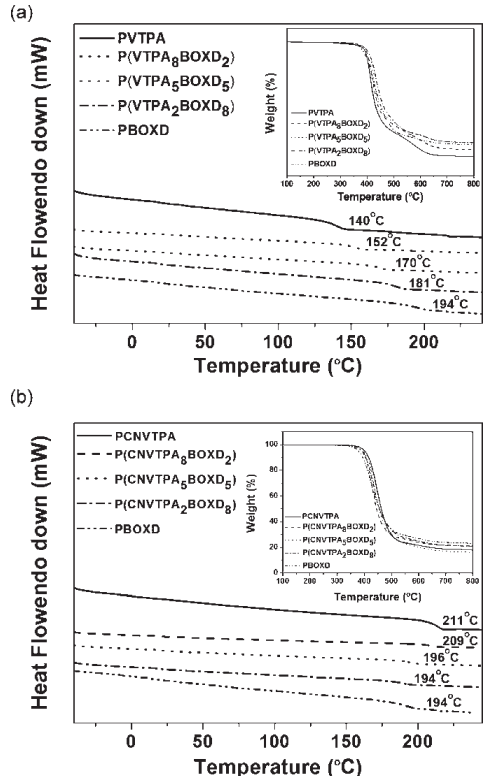

Figure 2. DSC thermograms of (a) PVTPA, PBOXD, and P(VTPA$_x$-BOXD$_y$) and (b) PCNVTPA, PBOXD, and P(CNVTPA$_x$BOXD$_y$) at a heating rate of 20 °C/min under nitrogen. The inset shows the TGA curves of all polymers with a heating rate of 20 °C/min under nitrogen.

respectively, similar to those of the PVTPA and PBOXD homopolymers. The ^{1}H NMR spectra of the other copolymers also exhibit essentially identical peak signals and are consistent with the proposed structures, as shown in Figures S1 and S2 of the Supporting Information. Because of the mixed proton signals of the random copolymers, it is difficult to estimate the relative D/A ratio directly from the peak integration of NMR spectra. Therefore, the different pendent D/A ratios of the prepared copolymers are further confirmed by elemental analysis. As described in synthesis part of the Experimental Section, the obtained carbon, hydrogen, and nitrogen contents are in a fair agreement with the theoretical values. It suggests that the pendent donor/acceptor ratios of the synthesized random copolymers are close to the original relative feeding of monomers. The synthesized P(VTPA$_x$BOXD$_y$) random copolymers exhibited good solubility in common organic solvents such as tetrahydrofuran (THF), chloroform, and chlorobenzene. However, P(CNVTPA$_x$BOXD$_y$) are only soluble in highly polar aprotic solvents such as dimethylformamide (DMF) or dimethylacetamide (DMAc). The weight-average molecular weights (M_w) of copolymers range from 12 700 to 29 600 with the polydispersity index (PDI) in the range of 1.17−1.37, determined by GPC analysis with polystyrene as standards.

Thermal Properties. The thermal properties of the polymers studied by DSC and TGA are shown in Figure 2 and summarized in Table 1. As exhibited in the inset of Figure 2, the thermal decomposition temperatures (T_d, 95 wt % residual) of the P(VTPA$_x$BOXD$_y$) and P(CNVTPA$_x$BOXD$_y$) random copolymers under flowing nitrogen are 392−395 and 390−396 °C, respectively. The DSC curves of the homopolymers, PVTPA, PCNVTPA, and PBOXD, have only single glass transition temperatures (T_g) at 140, 211, and 194 °C, respectively. On the other hand, all the T_g of random copolymers are observed in a range of 152−209 °C, which lie between the parent pendent donor and acceptor homopolymer. The better thermal properties of PCNVTPA than those of PVTPA can be attributed to the introduction of the cyano substituents, thereby increasing the rigidity of the pendant triphenylamine.[43] The high T_d and T_g of the pendent donor−acceptor random copolymers particularly suggest their applications for long-term stability of device operation.

Optical Properties. Figure 3 shows the UV−vis absorption spectra of the studied polymer thin films, and the corresponding absorption maxima (λ_{max}^{abs}) are summarized in Table 1. The absorption peak maxima in the spectra of PVTPA (306 nm) and PCNVTPA (shoulder peak) are assigned to the $\pi-\pi^*$ transition of the TPA moiety. The PCNVTPA absorbs up to a higher wavelength, probably due to the intramolecular charge transfer between the pendent TPA and cyano substituents. The weak absorption tail developed in the region between 400 and 600 nm is probably originally from interchain aggregation formation. Besides, the spectrum of PBOXD film has one strong-resolved absorption peak at 311 nm due to the $\pi-\pi^*$ transition of the aromatic ring. The absorption bands of P(VTPA$_x$BOXD$_y$) random copolymers with different molar ratios exhibit only one single maximum peak around 301−311 nm and appear between that of PVTPA and PBOXD homopolymers. However, the UV−vis spectra of P(CNVTPA$_x$BOXD$_y$) random copolymers show the increase in the BOXD absorption band with the BOXD composition, which roughly match the linear combination of the homopolymer spectra. The optical band gaps of PVTPA, PCNVTPA, PBOXD, P(VTPA$_x$BOXD$_y$), and P(CNVTPA$_x$BOXD$_y$) estimated from the absorption edges are 3.52, 3.08, 3.40, 3.40−3.52, and 3.11−3.14 eV, respectively. Besides, the random copolymers with different pendent donor/acceptor ratios do not exhibit obvious significant red shift or new absorption band, suggesting that the intramolecular charge transfer between the pendent TPA donor and the 1,3,4-oxadiazole acceptor is relatively weak.

Electrochemical Characteristics. The electrochemical behaviors of the synthesized polymer films investigated by cyclic voltammetry (CV) are summarized in Table 1. The oxidation−reduction behaviors of the prepared film were conducted on an ITO glass substrate in anhydrous acetonitrile or DMF containing 0.1 M TBAP under nitrogen that assembled in the three-electrode cells. According to the CV of the Figure 4, the P(VTPA$_8$BOXD$_2$) copolymer shows an irreversible oxidation behavior with the first oxidation peak at 1.32 eV on the first cycle. But, the appearance of lower onset oxidation potential on the second or third cycles of CV sweeps. It indicates that the TPA radicals perhaps undergo dimerization upon electrochemical oxidation, which is consistent with the literature.[52] However, the completely reversible oxidation behavior is observed in the P(CNVTPA$_8$BOXD$_2$) film. The radical cations derived from P(CNVTPA$_8$BOXD$_2$) are stable whereas the P(CNVTPA$_5$BOXD$_5$) or P(CNVTPA$_2$BOXD$_8$) copolymers and P(CNVTPA) homopolymer also exhibit similar reversible oxidation conditions, as shown in Figures S3 and S4 (Supporting Information). Besides, all the P(VTPA$_x$BOXD$_y$) and P(CNVTPA$_x$BOXD$_y$) copolymers and PBOXD homopolymer have reduction peaks from the pendent BOXD moiety in the range of −1.71 to −1.76 eV, as shown in Figures S4 and S5 (Supporting Information). The HOMO and LUMO energy levels of the random copolymers and homopolymers were estimated from CV with reference to ferrocene (4.8 eV) by the following equations: −LUMO = (E_{red}^{onset} vs Ag/AgCl +

Table 1. Thermal, Optical, and Electrochemical Properties of the Studied Homopolymers and Random Copolymers

			film		E/V (vs Ag/AgCl in MeCN or DMF)[c]			
index	T_g (°C)	T_d (°C)[a]	λ_{max}	E_g[b] (eV)	E_{ox}	E_{re}	HOMO[d] (eV)	LUMO[d] (eV)
PVTPA	140	397	306	3.52	0.99	NA	−5.35	−1.83
PCNVTPA	211	401	355	3.08	1.27	NA	−5.63	−2.55
PBOXD	194	378	311	3.40	NA	−1.74	−5.95	−2.55
P(VTPA$_8$BOXD$_2$)	152	395	306	3.52	0.98	−1.72	−5.34	−2.57
P(VTPA$_5$BOXD$_5$)	170	394	308	3.50	0.97	−1.71	−5.33	−2.58
P(VTPA$_2$BOXD$_8$)	181	392	311	3.40	0.96	−1.71	−5.32	−2.58
P(CNVTPA$_8$BOXD$_2$)	209	396	330	3.11	1.27	−1.76	−5.63	−2.53
P(CNVTPA$_5$BOXD$_5$)	196	394	330	3.13	1.28	−1.74	−5.64	−2.55
P(CNVTPA$_2$BOXD$_8$)	194	390	330	3.14	1.25	−1.73	−5.61	−2.56

[a] Thermal decomposition temperature (5% weight loss). [b] The data were calculated by the equation gap = $1240/\lambda_{onset}$ of monomer and polymer film. [c] Versus Ag/AgCl in CH_3CN (oxidation), vs Ag/AgCl in DMF (reduction). [d] The HOMO energy levels were calculated from cyclic voltammetry and were referenced to ferrocene (4.8 eV).

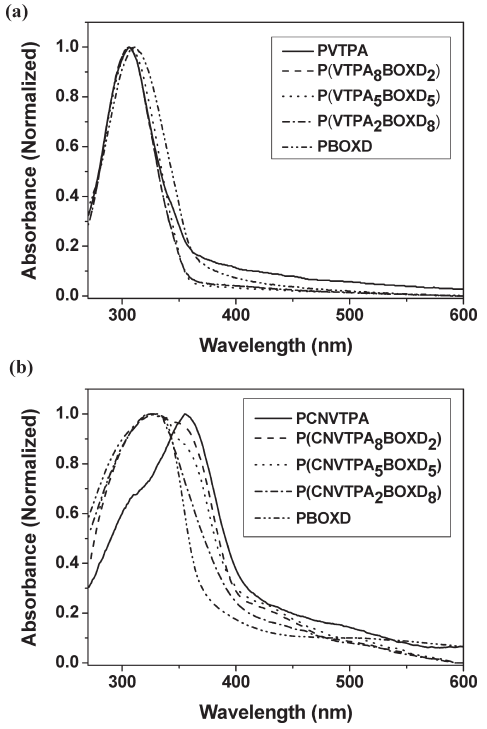

Figure 3. (a) Normalized UV−vis absorption spectra of (a) PVTPA, PBOXD, and P(VTPA$_x$BOXD$_y$) and (b) PCNVTPA, PBOXD, and P(CNVTPA$_x$BOXD$_y$) thin films on quartz plate.

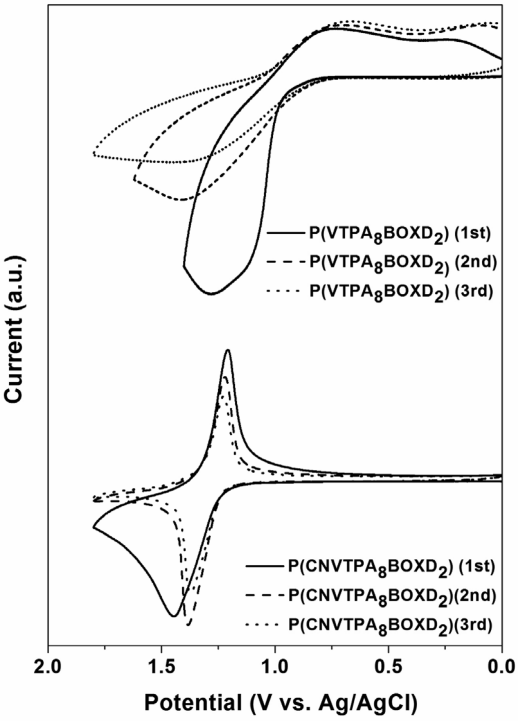

Figure 4. Cyclic voltammograms on oxidation scan of the spin-coated P(VTPA$_8$BOXD$_2$) and P(CNVTPA$_8$BOXD$_2$) thin films on an ITO glass substrate in CH_3CN containing 0.1 M TBAP at scan rate of 0.1 V/s.

4.8 eV − $E_{1/2}$, ferrocene); −HOMO = (E_{ox}^{onset} vs Ag/AgCl + 4.8 eV − $E_{1/2}$, ferrocene). In the CV scan, the PVTPA (or PCNVTPA) and PBOXD homopolymers only show anodic and cathodic peak at 0.99 V (or 1.27 V) and −1.74 V, respectively, which is corresponding to the HOMO level of −5.35 eV (or −5.63 eV) and LUMO level of −2.55 eV, respectively. The cathodic peak is not detected in the CV of PVTPA and PCNVTPA, and thus the LUMO level is taken from the difference between the HOMO level and optical band gap. The HOMO levels of PBOXD at −6.08 eV is also similarly determined. The stabilization of frontier orbtials of PCNVTPA compared to those of PVTPA is attributed to the introduction of the strong electron-withdrawing cyano-substituted group. The CV of P(VTPA$_x$BOXD$_y$) and P(CNVTPA$_x$BOXD$_y$) random copolymers show both p-doping and n-doping behavior, as shown in Figures S3 and S5 (Supporting Information). The HOMO energy levels of the copolymers with different D/A ratios are almost located at −5.35 eV (or −5.63 eV) from the electron-donating tendency of VTPA (or CNVTPA) units, whereas the LUMO energy levels of P(VTPA$_x$BOXD$_y$) copolymers are located at −2.55 eV from the electron-accepting tendency of BOXD. Here, the HOMO level of PVTPA homopolymer and P(VTPA$_x$BOXD$_y$) copolymers were calculated from oxidation peak in the first cycle. Therefore, the HOMO and LUMO energy levels of the random copolymers are similar to the corresponding pendent donor and acceptor homopolymers, respectively. Again, it indicates the relatively weak interaction between randomly pendent donor and acceptor from the electrochemical results.

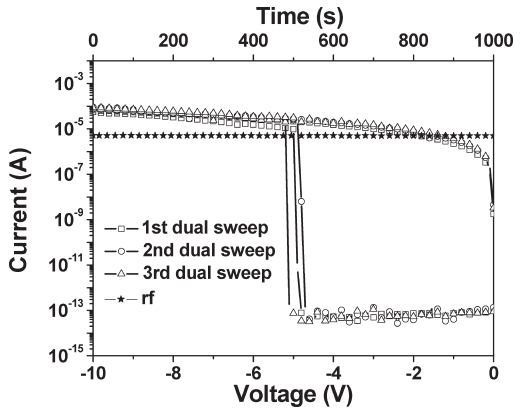

Figure 5. $I-V$ characteristic of P(VTPA$_8$BOXD$_2$) memory device in a dual-sweep mode.

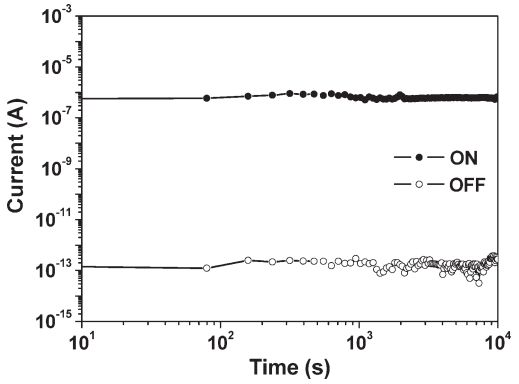

Figure 6. Retention time test on the ON and OFF states of the ITO/P(VTPA$_8$BOXD$_2$)/Al device under a continuous readout voltage.

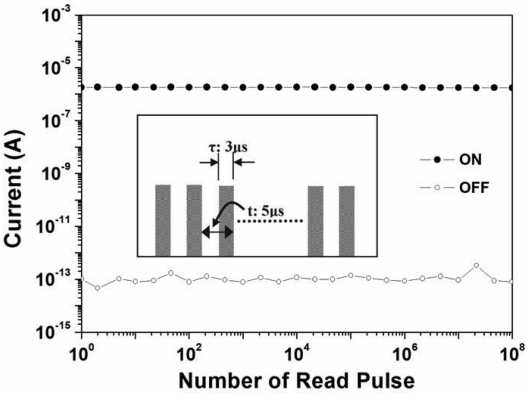

Figure 7. Stimulus effect of read pulses on the ON and OFF states of the ITO/P(VTPA$_8$BOXD$_2$)/Al device. The inset shows the pulse shapes in the measurement.

Memory Device Characteristics. The electrical behaviors were tested by the current−voltage ($I-V$) characteristics on the ITO/polymers/Al sandwiched device. Al was used as the anode (applied voltage bias), and ITO was set as the cathode (maintained as common) through the measurements.

Figure 5 shows the typical results of $I-V$ measurements for the P(VTPA$_8$BOXD$_2$) cells in steps of 0.1 V. The resistive memory devices store data based on the high- (ON) and low-conductance (OFF) response to the external applied voltages. A bias voltage is applied to the top Al electrode and swept dually from 0 V to −10 V to 0 V with a current compliance of 0.01 A, as shown in Figure 5. Besides, the voltage sweep from measuring instrument (Keithley 4200-SCS) is selected in a normal speed. The $I-V$ curves of P(VTPA$_8$BOXD$_2$) for three consecutive sweep cycles are reported. The devices initially exhibit a low current of $10^{-13}-10^{-12}$ A, which represents as the OFF state ("0" signal in data storage). The measurement in low-current region is pretty slowly (roughly 2 s each point). As a negative bias voltage is applied, the current of the cell suddenly changes to higher current state at a threshold voltage bias of −4.9 V, corresponding to the transition from OFF state to ON state. This electronic transition in the first negative sweep serves as the "writing" process. However, after the device switches to ON state, the current is recorded speedily (less than 2 s) from −10 to 0 V. The memory device can be kept on the ON state during the back sweep. Subsequent application of the second scan performed after turning off power for about 3 min can be reprogrammed from OFF state to ON state at −4.8 V again, and the current is kept in the ON state. It can be seen that an ON/OFF current ratio of 10^8 is obtained. For following testing cycles, the $I-V$ curves suggest that the ON state could be sustained for only a period of 3−5 min after turning off the power and would gradually relax back to the initial state. The OFF state can be further recovered to a stored state again with a small variation on reapplied switching voltage bias probably due to the delay on conformation changes of the pendent aromatic ring under the voltage bias. Thus, the short retention ability on the formation of high conductance channel between two electrodes in the P(VTPA$_8$BOXD$_2$) device reveals the common characteristics as a static random access memory (SRAM) feature since a temporary data remanence behavior is observed. Moreover, the volatile P(VTPA$_8$BOXD$_2$) device can be repeated for at least five continuous sweeps in the same cell or five different devices with reproducible data. This unstable ON state of the volatile memory device can also be retained by a refreshing voltage pulse of −1 V within 1 ms duration in every 5 s (named the rf trace in Figure 5). However, for further higher contents of the BOXD moiety, the $I-V$ curves of P(VTPA$_5$BOXD$_5$) and P(VTPA$_2$BOXD$_8$) devices show only a low current in the range of $10^{-13}-10^{-10}$ A during the voltage sweeps as shown in Figure S6 (Supporting Information).

The stability of the memory effect was also evaluated under the same atmosphere. Figure 6 shows representative results of the retention time tests under a constants stress of −1 V for both the ON and OFF states of P(VTPA$_8$BOXD$_2$) device, respectively. As can be seen in the figure, if the device is switched to the ON state by applying a voltage of 5 V, the ON state can be maintained without obvious degradation for at least 10^4 s. When the ON state is back to the OFF state, the OFF state can also be persisted for the whole test period, and the ON/OFF current ratio is kept about 10^7. In addition, the stimulus effect of continuous read pulse with a read voltage of −1 V on the ON and OFF state was also investigated as shown in Figure 7. The inset in Figure 7 shows the pulse generation used in the measurement with a pulse period and width of 3 and 2 μs, respectively. The current response of P(VTPA$_8$BOXD$_2$) memory device is quite stable for over 10^8 continuous read pluses. Therefore, both ON and OFF states are conducted under the voltage stress and continuous pulse cycles.

Besides, the PVTPA and PBOXD homopolymers were also carried out as a reference. For the ITO/PBOXD/Al device featuring the homogeneous PBOXD surface, the $I-V$ characteristic exhibits a low current that increases slowly upon the applied

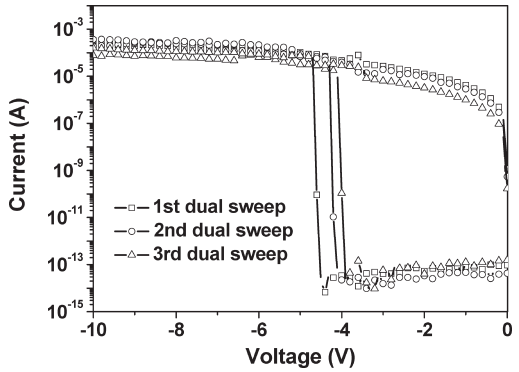

Figure 8. *I*−*V* characteristic of PVTPA memory device in a dual-sweep mode.

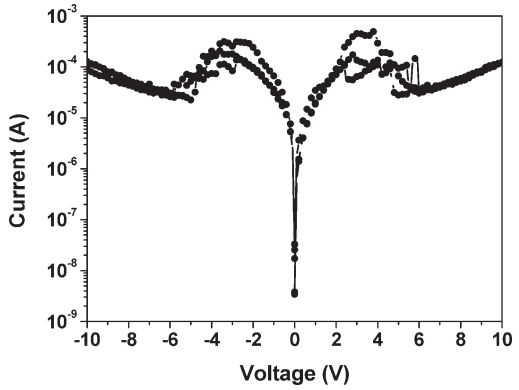

Figure 9. *I*−*V* characteristic of P(CNVTPA$_8$BOXD$_2$) memory device.

voltage bias, indicating that PBOXD shows an insulating state (Figure S6 of Supporting Information). In contrast, the ITO/PVTPA/Al device measured in dual-sweep mode with a negative bias (0 V to −10 V to 0 V) exhibits the electrical bistability with a sufficient large sensing margin up to 10^8, as shown in Figure 8. In the first dual sweep, there is an abrupt increase in the current near −4 V, which indicates that the film undergoes an electrical transition. As soon as the first sweep is completed (usually less than 20 s), the current state has relaxed to the OFF state. However, the OFF state can be further recovered to a stored state again with a reapplied switching voltage bias (second or third dual sweep), indicating that this device is also rewritable. Overall, ITO/PVTPA/Al device exhibits unique DRAM characteristics during the negative scan.

Meanwhile, the electrical characteristics of the PCNVTPA homopolymer and P(CNVTPA$_x$BOXD$_y$) copolymers device were systematically investigated. Figure 9 shows the *I*−*V* curves for P(VTPA$_8$BOXD$_2$) device at the same sweeping conditions. In the case of first sweep, the current reaches a maximum, then decreases with increasing voltage, and finally follows a monotonic region. It is noted that the back curve follows the same route. The N-shaped curve that contains the local current maximum (at −3 V; defined as maximum voltage (V_{max})) and minimum (at −5 V; defined as minimum voltage (V_{min})) is called negative differential resistance (NDR). Also, the current ratio between these two conductance states in the NDR region is ∼10. In the electrical scans of other polymers, PCNVTPA, P(VTPA$_5$BOXD$_5$), and P(VTPA$_2$BOXD$_8$), similar nonvolatile

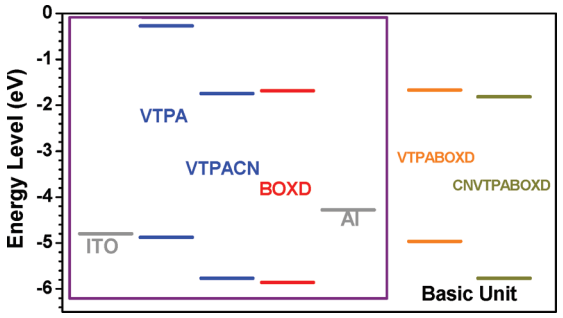

Figure 10. Molecular simulation of HOMO and LUMO energy levels for the VTPA, CNVTPA, and BOXD moieties and basic units of P(VTPA$_x$BOXD$_y$) and P(CNVTPA$_x$BOXD$_y$) along with the work function of the electrodes.

NDR properties are observed, as shown in the Figures S7−S9 (Supporting Information).

Operating Mechanism of Polymers Memory Device. The above volatile P(VTPA$_8$BOXD$_2$) copolymers and PVTPA homopolymer based devices may be due to the formation of the trapping level in the device and can be rationalized by evaluating the electronic structures on basic units of random copolymers. As shown in Figure 10, theoretical electronic calculations on the donor or acceptor moieties and basic unit of random copolymers were carried out by DFT/B3LYP/6-31G(d) with Gaussian 03 software. The absorption and CV results indicate that there is no obvious CT interaction between the pendent donor and acceptor moieties, which is also confirmed by our theoretical calculation. In terms of the HOMO and LUMO energy levels of polymers combined with work functions of ITO and Al, the energy barrier to the hole injection from ITO to the active memory layer (HOMO level of polymer) is absolutely smaller than energy barrier to the electron injection from Al to the active memory layer (LUMO level of polymer). Thus, it is easier for current flow when the ITO is enriched with holes (the top electrode is applied with negative bias). The materials based on TPA moieties are viewed as the hole transport media, and the hole mobility of PVTPA homopolymer measured from transistor device is about 10^{-7}−10^{-5} cm^2/(V s).[53] However, it is possible that the dimerization of the pendent TPA moiety creates the new high-lying HOMO band or unexpected defects can act as traps for hole transport within the films.[14,22,52,54] The charge is injected from the electrode into the materials, driven along the neighboring TPA and trapped in the polymer layer by the external electronic field. With further increase in bias voltage, the traps are filled and the current of the materials switches to a high value. The ON state cannot be maintained without a continuous voltage bias, and it returns to the original state soon after the removal of the applied electric field. The spontaneous back-transfer of the shallow trapped charges leads to the DRAM memory performance.[40]

Charge transport procedures occurred in the P(VTPA$_x$BOXD$_y$) films make the device become either unstable switching or insulating behavior. The incorporation of the electron-accepting BOXD group can serve as the hole-blocking moiety in the active memory layer due to its low-lying HOMO level.[36] Only limited charge transport occurs to make the sudden junction for current response. For the case of P(VTPA$_8$BOXD$_2$) device with a higher TPA donor content, the electrical switching exhibits the volatile memory behavior. Under the voltage bias near the threshold voltage, the sufficient generated charge can be filled into the

trapping environment, and the device switches from OFF to ON state with a continuous current flow. The longer holding period of the ON state (but still volatile) of P(VTPA$_8$BOXD$_2$) device relative to that of PVTPA device may due to the additional BOXD moiety that delay the back transferring of trapped hole process. Note that this trapping barrier of PVTPA from difference between the HOMO of the VTPA moiety and dimerized product is perhaps more shallow than that of the VTPA moiety and BOXD moiety. Besides, the slightly higher threshold voltages of P(VTPA$_8$BOXD$_2$) as compared to the PVTPA device may be attributed to the deeper HOMO level of BOXD in the film for the effective charge carrier transport. On the other hand, with increasing the BOXD ratio in the copolymers, the $I-V$ electrical curves of P(VTPA$_5$BOXD$_5$) and P(VTPA$_2$BOXD$_8$) devices work like an insulator, which is similar to the PBOXD homopolymer. Hole transport process between VTPA/BOXD moieties is completely blocked by the electron-accepting BOXD moiety in the film. A similar trend of the electrical characteristics with the donor/acceptor compositions of PVTPA/BOXD blend films is also observed, as shown in Figures S10−S12 of the Supporting Information. However, the film quality of the blend film is poorer than that of the copolymer film (Figure S13 of the Supporting Information), leading to variations of threshold voltage or current response.

By adding the cyano substituent to the TPA moiety, nonvolatile NDR memory devices are observed in all PCNVTPA and P(CNVTPA$_x$BOXD$_y$) devices, which are similar to the memory phenomena of thin insulating SiO$_x$ film observed by Simmons and Verderber.[55] The unfavorable dimerization of the TPA moiety is avoided by the cyano substituent, and the possibility of formation of traps from dimerization with the voltage bias may be excluded. Here, NDR behavior of PCNVTPA-based devices can be explained from the inclusion of Al particles into the organic polymer layer during the evaporation of top electrode as suggested previously.[56−59] It was reported that the Al atoms preferentially interact with the cyano groups.[60] Therefore, the Al metal can possibly diffuse into the polymer layer with sufficient thermal energy and serve as the deep charge trapping center. Initially, the current may be dominated by charge injection and tunneling process between the Al particles entrapping in the active layer. The charge starts to capture in the trapping site at the bias around the V_{max} and further charge trapping between tunneling sites reduce the current in the NDR region. The charge detrapping in the higher bias can subsequently lead to an increasing current along the pathway. Therefore, the Al diffusion into the polymer layer may lead to the NDR behavior in all PCNVTPA-based devices even in the higher BOXD content.

From the discussion above, the electrical properties of pendent polymers containing electron-rich TPA moieties can be modified via the electron-deficient group (such as BOXD or cyano substituents) for tuning the memory switching characteristics. Electric-field-induced electrical switching behaviors based on TPA donor−acceptor random copolymers can be expected to depend on charge transporting ability with coexisting charge trapping environment. The introduction of cyano substituents into the para position of TPA unit makes the presence of Al diffusion phenomenologically. Under such circumstances, P(CNVTPA$_x$-BOXD$_y$) random copolymers devices exhibit N-shaped $I-V$ characteristics with NDR region during the voltage scan. Hence, the electrical memory switching properties can be highly related to the choice of the polymer backbone.

CONCLUSIONS

We have successfully prepared new donor−acceptor random copolymers P(VTPA$_x$BOXD$_y$) or P(CNVTPA$_x$BOXD$_y$) containing pendent electron-donating TPA or dicyano-TPA and electron-accepting 1,3,4-oxadiazole via nitroxide-mediated free radical polymerization. The P(VTPA$_8$BOXD$_2$) and PVTPA device exhibited SRAM and DRAM switching, respectively, with an ON/OFF current ratio of 10^7-10^8. However, no switching phenomena were observed for a higher BOXD ratio. The electrical volatile nature is mainly attributed to charge transport and trapping/back-transferring of trapped charges. Moreover, the devices could endure 10^8 cycles under a pulse voltage and show long retention time of for at least 10^4 s under a constant voltage stress. On the other hand, the PCNVTPA and P(CNVTPA$_x$BOXD$_y$) memory device exhibited nonvolatile NDR behavior probably due to formation of Al atoms inside the polymer active layer originally from the incorporation of the cyano substituent. Our results open the molecular design of the pendent polymers with specific functional D−A chromopheres for advanced memory applications.

ASSOCIATED CONTENT

Supporting Information. Chemical structures and synthesis procedure of homopolymers; ^{1}H NMR spectra of P(VTPA$_5$BOXD$_5$), P(VTPA$_2$BOXD$_8$), P(CNVTPA$_8$OXD$_2$), P(CNVTPA$_5$OXD$_5$), and P(CNVTPA$_2$OXD$_8$) in CD_2Cl_2; CV on oxidation scan of P(VTPA$_5$BOXD$_5$), P(VTPA$_2$BOXD$_8$), P(CNVTPA$_5$BOXD$_5$), and P(CNVTPA$_2$BOXD$_8$) film; CV on reduction scan of P(VTPA$_x$BOXD$_y$) and P(CNVTPA$_x$BOXD$_y$) film; $I-V$ characteristics of P(VTPA$_5$BOXD$_5$), P(VTPA$_2$-BOXD$_8$), P(CNVTPA$_5$BOXD$_5$), P(CNVTPA$_2$BOXD$_8$), PBOXD, and PCNVTPA devices; $I-V$ characteristics of PVTPA/PBOXD blend (8/2, 5/5, and 2/8) film-based device; AFM images of P(VTPA$_8$BOXD$_2$), P(VTPA$_5$BOXD$_5$), and PVTPA/PBOXD blend (8/2 and 5/5) thin films. This material is available free of charge via the Internet at http://pubs.acs.org.

AUTHOR INFORMATION

Corresponding Author

*Tel: 886-2-3366-5236. Fax: 886-2-3366-5237. E-mail: chenwc@ntu.edu.tw.

Author Contributions

⊥Y. K. Fang and C. L. Liu equally contribute to this work.

ACKNOWLEDGMENT

Financial support of this work from the National Science Council, the Ministry of Economic Affairs, and the Excellence Research Program of National Taiwan University is highly appreciated. C. L. Liu also thanks for the financial support by Promotion of Environmental Improvement for Independence of Young Researchers Program of Ministry of Education, Culture, Sports, Science and Technology-Japan. The helpful discussion with Professor Moonhor Ree of Pohang University of Science and Technology is highly appreciated.

REFERENCES

(1) Liu, J.; Guo, X.; Bu, L. J.; Xie, Z. Y.; Cheng, Y. X.; Geng, Y. H.; Wang, L. X.; Jing, X. B.; Wang, F. S. *Adv. Funct. Mater.* **2007**, *17*, 1917.

(2) Wu, W. C.; Liu, C. L.; Chen, W. C. *Polymer* **2006**, *47*, 527.
(3) Baek, N. S.; Hau, S. K.; Yip, H. L.; Acton, O.; Chen, K. S.; Jen, A. K. Y. *Chem. Mater.* **2008**, *20*, 5734.
(4) Bijleveld, J. C.; Zoombelt, A. P.; Mathijssen, S. G. J.; Wienk, M. M.; Turbiez, M.; de Leeuw, D. M.; Janssen, R. A. *J. Am. Chem. Soc.* **2009**, *131*, 16616.
(5) Huo, L.; Hou, J.; Zhang, S.; Chen, H. Y.; Yang, Y. *Angew. Chem., Int. Ed.* **2010**, *49*, 1500.
(6) Huang, F.; Chen, K. S.; Yip, H. L.; Hau, S. K.; Acton, O.; Zhang, Y.; Luo, J. D.; Jen, A. K. Y. *J. Am. Chem. Soc.* **2009**, *131*, 13886.
(7) Qin, R. P.; Li, W. W.; Li, C. H.; Du, C.; Veit, C.; Schleiermacher, H. F.; Andersson, M.; Bo, Z. S.; Li, Z. P.; Liu, Z. P.; Inganas, O.; Wuerfel, U.; Zhang, F. L. *J. Am. Chem. Soc.* **2009**, *131*, 14612.
(8) Duan, C. H.; Chen, K. S.; Huang, F.; Yip, H. L.; Liu, S. J.; Zhang, J.; Jen, A. K. Y.; Cao, Y. *Chem. Mater.* **2010**, *22*, 6444.
(9) Yuan, M. C.; Chiu, M. Y.; Liu, S. P.; Chiang, C. M.; Wei, K. H. *Macromolecules* **2010**, *43*, 6934.
(10) Yuan, M. C.; Chiu, M. Y.; Chiang, C. M.; Wei, K. H. *Macromolecules* **2010**, *43*, 6270.
(11) Liu, C. L.; Tsai, J. H.; Lee, W. Y.; Chen, W. C.; Jenekhe, S. A. *Macromolecules* **2008**, *41*, 6952.
(12) Tsai, J. H.; Chueh, C. C.; Lai, M. H.; Wang, C. F.; Chen, W. C.; Ko, B. T.; Ting, C. *Macromolecules* **2009**, *42*, 1897.
(13) Wu, P. T.; Bull, T.; Kim, F. S.; Luscombe, C. K.; Jenekhe, S. A. *Macromolecules* **2009**, *42*, 671.
(14) Tsai, J. H.; Chueh, C. C.; Chen, W. C.; Yu, C. Y.; Hwang, G. W.; Ting, C.; Chen, E. C.; Meng, H. F. *J. Polym. Sci., Polym. Chem.* **2010**, *48*, 2351.
(15) Tsai, J. H.; Lee, W. Y.; Chen, W. C.; Yu, C. Y.; Hwang, G. W.; Ting, C. *Chem. Mater.* **2010**, *22*, 3290.
(16) Becerril, H. A.; Miyaki, N.; Tang, M. L.; Mondal, R.; Sun, Y. S.; Mayer, A. C.; Parmer, J. E.; McGehee, M. D.; Bao, Z. *J. Mater. Chem.* **2009**, *19*, 591.
(17) Cheng, K. F.; Liu, C. L.; Chen, W. C. *J. Polym. Sci., Polym. Chem.* **2007**, *45*, 5872.
(18) Babel, A.; Zhu, Y.; Cheng, K. F.; Chen, W. C.; Jenekhe, S. A. *Adv. Funct. Mater.* **2007**, *17*, 2542.
(19) Ling, Q. D.; Liaw, D. J.; Zhu, C.; Chan, D. S. H.; Kang, E. T.; Neoh, K. G. *Prog. Polym. Sci.* **2008**, *33*, 917.
(20) Ling, Q. D.; Liaw, D. J.; Teo, E. Y. H.; Zhu, C.; Chan, D. S. H.; Kang, E. T.; Neoh, K. G. *Polymer* **2007**, *48*, 5182.
(21) Scott, J. C.; Bozano, L. D. *Adv. Mater.* **2007**, *19*, 1452.
(22) Thelakkat, M. *Macromol. Mater. Eng.* **2002**, *287*, 442.
(23) Shirota, Y.; Kageyama, H. *Chem. Rev.* **2007**, *107*, 953.
(24) Ling, Q. D.; Chang, F. C.; Sang, Y.; Zhu, C. X.; Liaw, D. J.; Chan, D. S. H.; Kang, E. T.; Neoh, K. G. *J. Am. Chem. Soc.* **2006**, *128*, 8732.
(25) Lee, T. J.; Chang, C. W.; Hahm, S. G.; Kim, K.; Park, S.; Kim, D. M.; Kim, J.; Kwon, W. S.; Liou, G. S.; Ree, M. *Nanotechnology* **2009**, *20*, 135204.
(26) Kim, K.; Park, S.; Hahm, S. G.; Lee, T. J.; Kim, D. M.; Kim, J. C.; Kwon, W.; Ko, Y. G.; Ree, M. *J. Phys. Chem. B* **2009**, *113*, 9143.
(27) You, N. H.; Chueh, C. C.; Liu, C. L.; Ueda, M.; Chen, W. C. *Macromolecules* **2009**, *42*, 4456.
(28) Wang, K. L.; Liu, Y. L.; Lee, J. W.; Neoh, K. G.; Kang, E. T. *Macromolecules* **2010**, *43*, 7159.
(29) Zhang, X. D.; Chen, Y.; Liu, G.; Li, P. P.; Zhu, C. X.; Kang, E. T.; Neoh, K. G.; Zhang, B.; Zhu, J. H.; Li, Y. X. *Adv. Mater.* **2010**, *22*, 1731.
(30) Sommer, M.; Linder, S. M.; Thelakkat, M. *Adv. Funct. Mater.* **2007**, *17*, 1493.
(31) Huttner, S.; Sommer, M.; Chiche, A.; Krausch, G.; Steiner, U.; Thelakkat, M. *Soft Matter* **2009**, *5*, 4206.
(32) Behl, M.; Zentel, R. *Macromol. Chem. Phys.* **2004**, *205*, 1633.
(33) Tsuchiya, K.; Kasuga, H.; Kawakami, A.; Taka, H.; Kita, H.; Ogino, K. *J. Polym. Sci., Polym. Chem.* **2010**, *48*, 1461.
(34) You, N. H.; Chueh, C. C.; Liu, C. L.; Ueda, M.; Chen, W. C. *Macromolecules* **2009**, *42*, 4456.
(35) Fang, Y. K.; Liu, C. L.; Li, C.; Lin, C. J.; Mezzenga, R.; Chen, W. C. *Adv. Funct. Mater.* **2010**, *20*, 3012.
(36) Fang, Y. K.; Liu, C. L.; Cheng, W. C. *J. Mater. Chem.* **2011**, *21*, 4778.
(37) Hsu, J. C.; Liu, C. L.; Chen, W. C.; Sugiyama, K.; Hirao, A. *Macromol. Rapid Commun.* **2011**, *32*, 528.
(38) Ma, Y.; Cao, X.; Li, G.; Wen, Y.; Yang, Y.; Wang, J.; Du, S.; Yang, L.; Gao, H.; Song, Y. *Adv. Funct. Mater.* **2010**, *20*, 803.
(39) Li, H.; Xu, Q.; Li, N.; Sun, R.; Ge, J.; Lu, J.; Gu, H.; Yang, F. *J. Am. Chem. Soc.* **2010**, *132*, 5542.
(40) Ling, Q. D.; Song, Y.; Lim, S. L.; Teo, E. Y. H.; Tan, Y. P.; Zhu, C.; Kang, E. T.; Neoh, K. G. *Angew. Chem., Int. Ed.* **2006**, *45*, 2947.
(41) Baek, S.; Lee, D.; Kim, J.; Hong, S. H.; Kim, O.; Ree, M. *Adv. Funct. Mater.* **2007**, *17*, 2637.
(42) Zhuang, X. D.; Chen, Y.; Li, B. X.; Ma, D. G.; Zhang, B.; Li, Y. *Chem. Mater.* **2010**, *22*, 4455.
(43) Ling, Q.; Song, Y.; Ding, S. J.; Zhu, C.; Chan, D. S. H.; Kwong, D. L.; Kang, E. T.; Neoh, K. G. *Adv. Mater.* **2005**, *17*, 455.
(44) Lim, S. L.; Li, N. J.; Lu, J. M.; Ling, Q. D.; Zhu, C. X.; Kang, E. T.; Neoh, K. G. *ACS Appl. Mater. Interfaces* **2009**, *1*, 60.
(45) Ouyang, J.; Chu, C. W.; Szmanda, C. R.; Ma, L.; Yang, Y. *Nano Lett.* **2005**, *5*, 1077.
(46) Tseng, R. J.; Huang, J.; Ouyang, J.; Kaner, R. B.; Yang, Y. *Nature Mater.* **2004**, *3*, 918.
(47) Chu, C. W.; Ouyang, J.; Tseng, J. H.; Yang, Y. *Adv. Mater.* **2005**, *17*, 1440.
(48) Liu, G.; Ling, Q. D.; Teo, E. Y. H.; Zhu, C. X.; Chan, D. S. H.; Neoh, K. G.; Kang, E. T. *ACS Nano* **2009**, *3*, 1929.
(49) Lee, C. C.; Yen, K. M.; Chen, Y. *J. Poym. Sci., Polym. Chem.* **2008**, *46*, 7960.
(50) Fang, Y. K.; Lee, W. Y.; Tuan, C. S.; Lu, L. H.; Teng, W. J.; Chen, W. C. *Polym. J.* **2010**, *42*, 327.
(51) Frisch, M. J.; et al. *Gaussian 03, Revision B.04*; Gaussian, Inc.: Wallingford, CT, 2004.
(52) Compton, R. G.; Laing, M. E.; Ledwith, A.; Abu-Abdoun, I. I. *J. Appl. Electrochem.* **1988**, *18*, 431.
(53) Hüttner, S.; Sommer, M.; Steiner, U.; Thelakkat, M. *Appl. Phys. Lett.* **2010**, *96*, 073503.
(54) Seo, E. T.; Nelson, R. F.; Fritsch, J. M.; Marcoux, L. S.; Leedy, D. W.; Adams, R. N. *J. Am. Chem. Soc.* **1966**, *88*, 3498.
(55) Simmons, J. G.; Verderber, R. R. *Proc. R. Soc. London, Ser. A* **1967**, *301*, 77.
(56) Bozano, L. D.; Kean, B. W.; Beinhoff, M.; Carter, K. R.; Rice, P. M.; Campbell Scott, J. C. *Adv. Funct. Mater.* **2005**, *15*, 1933.
(57) Kondo, T.; Lee, S. M.; Malicki, M.; Domercq, B.; Marder, S. R.; Kippelen, B. *Adv. Funct. Mater.* **2008**, *18*, 1112.
(58) Chen, J.; Ma, D. *Appl. Phys. Lett.* **2005**, *87*, 023505.
(59) Lin, J.; Ma, D. *J. Appl. Phys.* **2008**, *103*, 124505.
(60) Fahlman, M.; Salaneck, W. R.; Moratti, S. C.; Holmes, A. B.; Brédas, J. L. *Chem.—Eur. J.* **1997**, *3*, 286.